

## SHEATH FLOW-CONTROLLED MOLECULAR DIFFUSION IN THREE DIMENSIONAL MULTIPLE MICRO-MIXER

E. LEE<sup>a</sup>, S. CHEUN CHOI<sup>b</sup>, J. OH<sup>c,d\*</sup>

<sup>a</sup>*Department of Bionanosystem Engineering, Chonbuk National University, Jeonju 561-756, South Korea*

<sup>b</sup>*Thermochemical Energy System R&BD Group, Korea Institute of Industrial Technology, Cheonan, Korea*

<sup>c</sup>*Hemorheology Research Institute, Chonbuk National University, Jeonju 561-756, South Korea*

<sup>d</sup>*Division of Mechanical Design Engineering, Chonbuk National University, Jeonju 561-756, South Korea*

We present a sheath flow-driven multiple micro-mixer for biological, pharmacological, and biochemical analyses. The glass capillary-based multiple micro-mixer was designed, fabricated, and tested to improve molecular diffusion. Rhodamine B solution (2.0 mol/m<sup>3</sup>), Brilliant blue solution (2.0 mol/m<sup>3</sup>), and deionized water (0 mol/m<sup>3</sup>) were infused into inlets. The experimental results were identical to those obtained from the simulations in that deionized water as a sheath flow could control the transport of Rhodamine B and Brilliant blue by diffusion, resulting in an improvement in the multiple micro-mixing at the nano scale.

(Received March 8, 2015; Accepted May 9, 2015)

*Keywords:* Sheath flow; Micro-mixer; Molecular diffusion; Rhodamine B; Brilliant blue

### 1. Introduction

Mixing is performed at the microscale to transport molecules through at least two different phases of liquids, solids, or gases. Micro-mixing is an essential function that is required to effectively control micro- or nano-liter fluids for biological, pharmacological, and biochemical analysis due to the ability to provide a (1) very small mixing volume, (2) fast reaction time, and (3) homogenous mixing [1, 2].

Micro-mixing can be incorporated with microfluidic devices that provide a significant increase in performance for mixing. Microfluidics are defined as methods to manipulate fluid flows in the micro-sized length scale and their applicability has expanded to various areas in drug chemistry, biology, physics, and biomedical engineering [3-5]. This favorable attention toward microfluidics is a result of their (1) portability to conduct point-of-care diagnosis, (2) low fabrication cost for devices, (3) rapid development of biological manipulation devices on the scale of cells, (4) very small reagent consumption, and (5) quick integration of different microfluidic devices for multiple functionalities [3, 6].

Micro-mixing can be mainly categorized as active and passive mixing depending on the application of external forces. Active micro-mixing provides fast and homogenized mixing using electrokinetic-displaced stirring, acoustic-driven shaking, electrical field-based time-pulsing flow, and electrowetting-based oscillation [7-9]. In contrast, passive mixing does not require the use of any external forces but can nevertheless provide a homogeneous mixing through the use of specially-designed configurations. The key principle of passive micro-mixing is to increase the

---

\*Corresponding author: jonghyuno@jbnu.ac.kr

contact area and time between fluids using microfluidic techniques, such as twisted channels, embedded channels, zigzag channels, lamination, a three-dimensional serpentine structure, and surface chemistry technology [6, 7, 10]. When compared to active micro-mixing, passive micro-mixing has advantages in that it provides for cost-effective, simple fabrication of disposable platforms since it requires no additional devices to provide external force or to input energy.

In this study, a very simple and effective passive micro-mixer was introduced to conduct sheath flow-driven multiple micro-mixing to enhance molecular diffusion. A glass capillary-based microfluidic mixer could generate truly three-dimensional co-axial flows that enhance the efficacy of micro-mixing relative to two-dimensional microfluidic devices [11]. A computer-aided microfluidic simulation was performed to estimate the mixing performance of the micro-mixer as well as its chemical stability, and the precise control of multiple diffusion was demonstrated as a function of the sheath flow rate, and the results were visualized using two different dyes in water.

## 2. Experimental

### 2.1 Materials

A three-dimensional sheath flow-driven multiple micro-mixer was investigated using two dyes – Rhodamine B (MW = 479.01 g/mol; Sigma Aldrich, MO, USA) and Brilliant Blue G-250 (MW = 854.02 g/mol; Sigma Aldrich, MO, USA) – to visualize the micro-mixing process. 20.0 mg of Rhodamine B (RB) were mixed with 20 ml of deionized (DI) water to prepare Rhodamine B (RB) solution at a 2.0 mol/m<sup>3</sup> concentration. For the 2.0 mol/m<sup>3</sup> concentration of Brilliant Blue G-250 (BB) solution, 34.2 mg of Brilliant Blue G-250 were dissolved in 20 ml of deionized water. The two solutions were then filtered.

### 2.2 Design optimization of the micro-mixer

Fig. 1 shows a schematic of the sheath flow-driven multiple micro-mixer. We used the Comsol Multiphysics software to optimize the design and study the parameters prior to fabricating the micro-mixer. The simplified two-dimensional geometry of the multiple micro-mixer was modeled to conduct a finite-element-based analysis. The finite-element model consisted of three inlets and one outlet that used a glass capillary, as shown in Fig 1. For the microfluidic flow, two core inlet flows were generated by using RB and BB solutions infused by syringe pumps while the sheath flow with DI water was introduced into one large inlet.

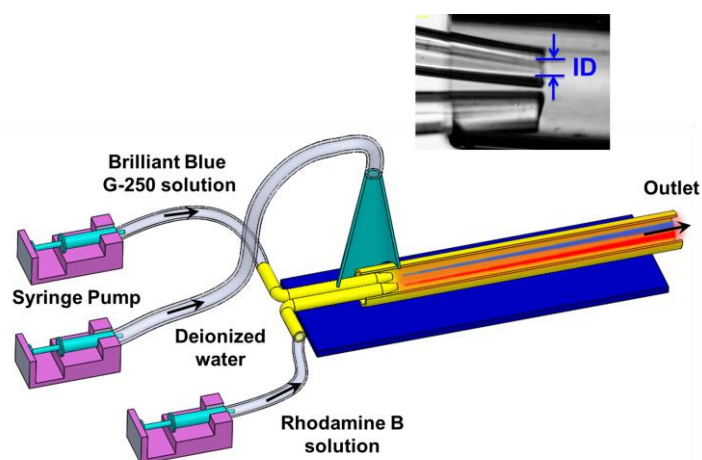


Fig. 1. (a) Schematic of the sheath flow-driven multiple micro-mixer (ID = 100  $\mu\text{m}$ ).

The multiple micro-mixing was analyzed by formulating a mathematical coupling of the fluid velocity field between the laminar flow model and the transport model of the diluted species.

The conservation of momentum and mass for the incompressible and laminar flow analyses were represented using Navier-Stokes and continuity equations, respectively, as follows.

$$\rho \frac{\partial \mathbf{u}}{\partial t} + \mathbf{u} \cdot \nabla \mathbf{u} = -\nabla p + \mu \nabla^2 \mathbf{u} + \mathbf{F} \quad (1)$$

$$\frac{\partial \rho}{\partial t} + \nabla \cdot (\rho \mathbf{u}) = 0 \quad (2)$$

where  $\rho$  is the density ( $\text{kg/m}^3$ ),  $\mathbf{u}$  is the velocity ( $\text{m/s}$ ),  $p$  is the pressure ( $\text{Pa}$ ),  $\mu$  is the dynamic viscosity ( $\text{Pa}\cdot\text{s}$ ), and  $\mathbf{F}$  is the volume force ( $\text{N/m}^3$ ). Equations (1) and (2) were solved with the inlet boundary conditions (RB flow rate = 500  $\mu\text{l/h}$ ; BB flow rate = 500  $\mu\text{l/h}$ ; DI water flow rate = 500 – 6,000  $\mu\text{l/h}$ ) and zero pressure at the outlet. The no-slip condition was applied on the wall, and the viscosities of the RB solution, BB solution, and DI water were considered to be equivalent.

The transport of diluted RB and BB via diffusion was studied using the chemical mass balance equation, accounting for diffusive interactions between the diluted species and the solvent (i.e., DI water):

$$\nabla \cdot (-D \nabla c) + \mathbf{u} \cdot \nabla c = R \quad (3)$$

where  $c$  denotes the concentration of the diluted species ( $\text{mol/m}^3$ ),  $D$  is the diffusion coefficient ( $\text{m}^2/\text{s}$ ),  $\mathbf{u}$  is the velocity vector ( $\text{m/s}$ ), and  $R$  indicates the reaction rate for species [ $\text{mol}/(\text{m}^3\cdot\text{s})$ ]. The diffusion equation (3) was solved with the inlet boundary conditions (RB concentration = 2.0  $\text{mol/m}^3$ ; BB concentration = 2.0  $\text{mol/m}^3$ ; DI water concentration = 0  $\text{mol/m}^3$ ). The symmetry wall was assumed to be insulated, and the diffusion coefficients of RB and BB into water were  $3.6 \times 10^{-10}$  and  $2.8 \times 10^{-9}$   $\text{m}^2/\text{s}$ , respectively [12, 13]. A physics-controlled mesh was optimally generated for the micro-mixing geometry to solve the coupled laminar flow and chemical transport model. The solutions were then properly post-processed to visualize the controlled multiple micro-mixing by diffusion.

### 2.3 Fabrication of co-axial multiple micro-mixer

The optimally-designed sheath flow-driven microfluidic device was fabricated with three inlets (RB, BB, and DI water) and one outlet. Fig. 1 shows two small inlets for RB and BB solutions made by bending 100- $\mu\text{m}$ -ID glass capillaries (World Precision Instruments, Inc., FL, USA). Here, the 100- $\mu\text{m}$ -ID glass capillaries were manually drawn (from ID = 580  $\mu\text{m}$  down to ID = 100  $\mu\text{m}$ ) under a thermal process, and two small inlets were inserted into the main glass capillary (ID = 1,000  $\mu\text{m}$ ) to generate a three-dimensional co-axial flow. The other inlet was prepared for DI water by using a pipette tip (10 – 100  $\mu\text{l}$ ) that was vertically aligned to the connection with the main glass capillary. Three glass capillaries and one pipette tip were permanently fixed on a slide glass (25 x 75 mm) using epoxy resin, and all the three inlets were connected to syringe pumps (Genie Touch, Kent Scientific, Inc., CT, USA) to provide a constant infusion. Three glass syringes (RB=3 ml, BB=3 ml, and DI water=5 ml) were then installed in the syringe pumps.

### 2.4 Experiment of co-axial multiple micro-mixing

The multiple micro-mixer that was fabricated tested by varying the flow rates of the DI water as sheath flow. The DI water was perfused into the main channel at flow rates ranging from 500 to 6,000  $\mu\text{l/h}$  while the RB and BB solutions were introduced into the micro-mixer at a constant flow rate of 500  $\mu\text{l/h}$ . The temperature of the experimental environment was maintained at  $21 \pm 1.0$   $^\circ\text{C}$  to eliminate the effect of the temperature variation on the diffusion. The multiple micro-mixing of RB, BB, and DI water were observed under an inverted optical microscope (Olympus, Tokyo, Japan).

### 3. Results and discussion

A finite element-aided simulation was used to design a sheath flow-driven multiple micro-mixer. Three different fluids (RB solution, BB solution, and DI water) were introduced into the micro-mixer through their respective inlets, and then the fluids were united in the main channel. The simulated model could maintain stable laminar streams at the inlets without any initial mixing, and therefore, DI water with zero molecular concentration stayed in its own stream while the RB and BB molecules with a  $2.0 \text{ mol/m}^3$  molecular concentration could be transported via diffusion.

Fig. 2 describes the effect of the sheath flow of DI water in terms of the improvement in molecular diffusion. Figs. 2(a) to (d) show a simulated concentration distribution of RB and BB solutions by changing the sheath flow rates from  $500 \text{ }\mu\text{l/h}$  to  $6,000 \text{ }\mu\text{l/h}$  at constant flow rates of RB and BB ( $500 \text{ }\mu\text{l/h}$ ). In Fig. 2(c), as the sheath flow rate decreased below  $4,000 \text{ }\mu\text{l/h}$ , a three dimensional co-axial defocusing flow was generated. The defocusing flows that were generated were laterally propagated along the flow direction. In contrast, in Fig. 2(d), as the sheath flow rate increased above  $4,000 \text{ }\mu\text{l/h}$ , the focusing flow was apparently developed, resulting in no significant internal or external diffusions. Interestingly, the sheath flow could control the performance of the multiple mixing as well as the flow stability at the micro scale.

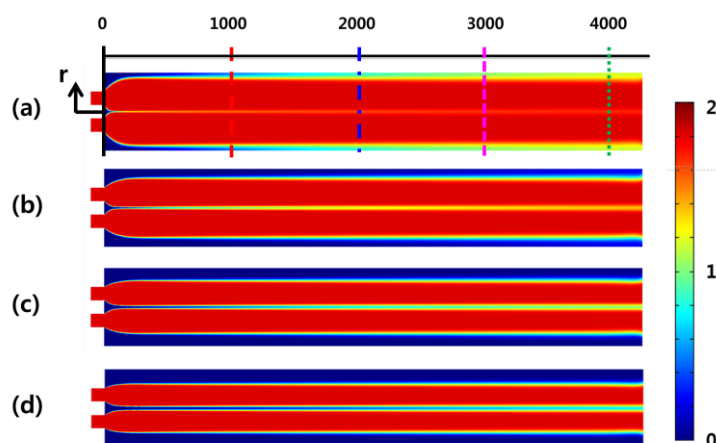


Fig. 2. Surface concentration distributions of Rhodamine B (RB;  $2.0 \text{ mol/m}^3$ ) and Brilliant blue (BB;  $2.0 \text{ mol/m}^3$ ) according to the sheath flow rates. The flow rates of the RB and BB solutions were constant at  $500 \text{ }\mu\text{l/h}$ . RB and BB concentration distributions at sheath flow rates of (a)  $500 \text{ }\mu\text{l/h}$ , (b)  $2,000 \text{ }\mu\text{l/h}$ , (c)  $4,000 \text{ }\mu\text{l/h}$ , and (d)  $6,000 \text{ }\mu\text{l/h}$ , respectively.

Fig. 3 describes the cross-sectional concentration profiles for RB and BB along the flow direction. The co-axial defocusing flow caused by the sheath flow accelerated the net flux of molecules, resulting in a concentration gradient along the flow direction [Fig. 3(b)]. The concentration gradient was inversely proportional to the sheath flow rate, and different molecular diffusion coefficients between RB and BB caused an asymmetric distribution in the concentration. The higher BB diffusion coefficient indicated a greater transport of molecules than the lower RB diffusion coefficient.

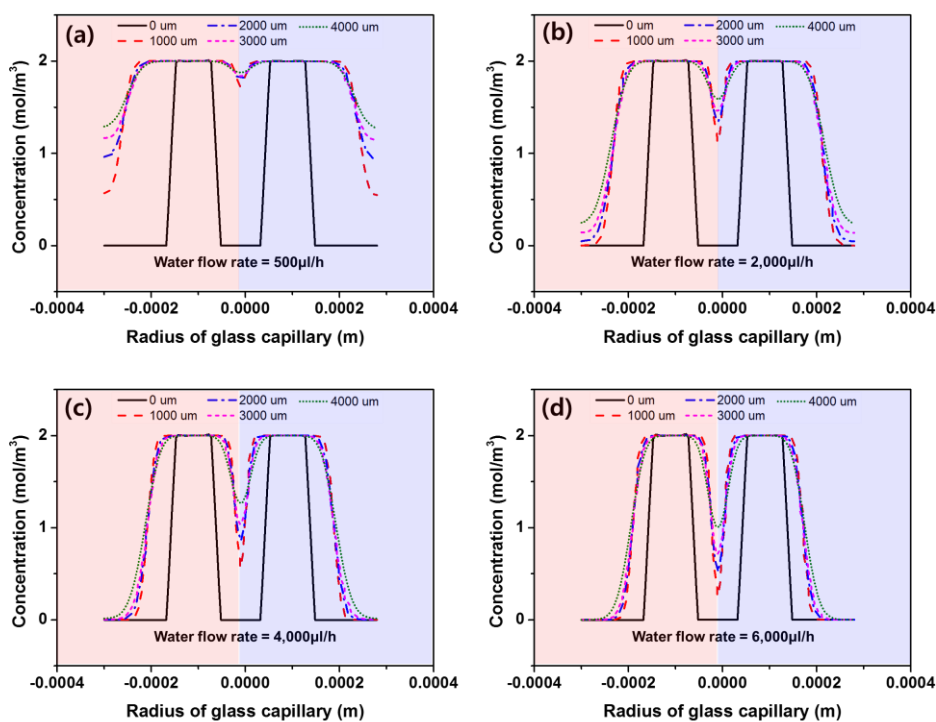
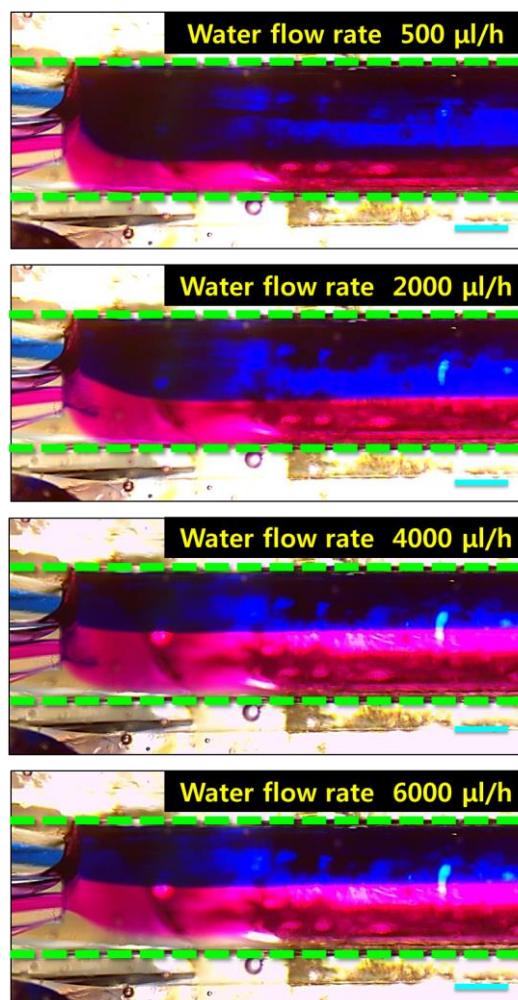


Fig. 3. Characterization of the molecular diffusion of RB and BB solutions as a function of the sheath flow rate. The cross-sectional concentration profiles of RB and BB solutions according to a distance of  $0\ \mu\text{m}$ ,  $1,000\ \mu\text{m}$ ,  $2,000\ \mu\text{m}$ ,  $3,000\ \mu\text{m}$ , and  $4,000\ \mu\text{m}$  from the inlet at a sheath flow rate of (a)  $500\ \mu\text{l/h}$ , (b)  $2,000\ \mu\text{l/h}$ , (c)  $4,000\ \mu\text{l/h}$ , and (d)  $6,000\ \mu\text{l/h}$ , respectively.

In Fig. 4, the sheath flow-driven multiple micro-mixer was fabricated and tested. DI water could be located as the sheath flow in the shell region of the co-axial flow while both the RB and BB flows were placed in the core region. By controlling the sheath flow rate from  $500\ \mu\text{l/h}$  to  $6,000\ \mu\text{l/h}$ , the transition between flow focusing and defocusing was observed as was predicted by the computer-aided simulation.



*Fig. 4. Experimental images of the molecular diffusion enhanced by the sheath flow-driven effect. A defocusing flow was generated below a sheath flow rate of 4,000  $\mu\text{l/h}$ , showing an improvement in molecular diffusion. Above a sheath flow rate of 4,000  $\mu\text{l/h}$ , the sheath flow caused a focusing flow, resulting in less molecule transport through diffusion.*

Multiple micro-mixing of the RB solution, BB solution, and DI water were characterized according to the controllable sheath flow rate. The red and blue areas indicate the RB and BB streams with different diffusion coefficients of  $3.6 \times 10^{-10}$  and  $2.8 \times 10^{-9}$   $\text{m}^2/\text{s}$ , respectively. The boundary profile between the two streams represents the degree of diffusion, and a critical situation was observed at a sheath flow rate of 4,000  $\mu\text{l/h}$ . Below the critical sheath flow rate, the lateral profile was biased towards the RB area, and the width of the lateral bias was inversely proportional to the sheath flow rate. However, no bias was observed above 4,000  $\mu\text{l/h}$ . The above-mentioned experimental results therefore indicate that the sheath flow could be closely correlated to the diffusive transport of different molecules for multiple micro-mixing.

#### **4. Conclusion**

A sheath flow-driven multiple micro-mixer was successfully designed, fabricated, and tested. A computer-aided simulation was performed in order to predict the performance of the micro-mixer, and the micro-mixer was then fabricated using micro glass capillaries. The micro-mixer was tested using an RB solution, BB solution, and DI water to visualize the molecular diffusion, and the results of the experiment are identical to those obtained from simulations to

show that the sheath flow could control and improve molecular diffusion for the multiple micro-mixing. The proposed sheath flow-driven multiple micro-mixer can be a promising tool for use with biological, pharmacological, and biochemical analyses with Lab-On-Chip devices and micro Total Analysis Systems.

### Acknowledgements

This research was supported by Basic Science Research Program through the National Research Foundation of Korea (NRF), funded by the Ministry of Education (NRF-2014R1A1A1006388 and NRF-2013R1A1A2058875).

### References

- [1] T.J. Johnson, D. Ross, L.E. Locascio, *Anal. Chem.*, **74**, 45 (2002).
- [2] N.-T. Nguyen, Z. Wu, *J. Micromech. Microeng.*, **15**, R1 (2005).
- [3] H.A. Stone, A.D. Stroock, A. Ajdari, *Annu. Rev. Fluid Mech.*, **36**, 381 (2004).
- [4] D.J. Beebe, G.A. Mensing, G.M. Walker, *Annu. Rev. Biomed. Eng.*, **4**, 261 (2002).
- [5] P.S. Dittrich, A. Manz, *Nat. Rev. Drug Discov.*, **5**, 210 (2006).
- [6] C.Y. Lee, C.L. Chang, Y.N. Wang, L.M. Fu, *Int. J. Mol. Sci.*, **12**, 3263 (2011).
- [7] V. Hessel, H. Löwe, F. Schönfeld, *Chem Eng Sci*, **60**, 2479 (2005).
- [8] M. Campisi, D. Accoto, F. Damiani, P. Dario, *J. Micro-Nano Mechatron.*, **5**, 69 (2009).
- [9] D. Ahmed, X. Mao, B.K. Juluri, T.J. Huang, *Microfluid. Nanofluid.*, **7**, 727 (2009).
- [10] C.Y. Lee, C. Lin, M. Hung, R. Ma, C.H. Tsai, C.H. Lin, L.M. Fu, *Mater. Sci. Forum*, **505**, 391 (2006).
- [11] S. Takeuchi, P. Garstecki, D.B. Weibel, G.M. Whitesides, *Adv Mater*, **17**, 1067 (2005).
- [12] P. Gendron, F. Avaltroni, K. Wilkinson, *J. Fluoresc.*, **18**, 1093 (2008).
- [13] C. Lin, C. Tsai, L. Fu, *J. Micromech. Microeng.*, **15**, 935 (2005).